LBNL-40415
UC-410
Preprint

ERNEST ORLANDO LAWRENCE
BERKELEY NATIONAL LABORATORY

Breakdown of the Independent Particle Approximation in High-Energy Photoionization

E.W.B. Dias, H.S. Chakraborty, P.C. Deshmukh, S.T. Manson, O. Hemmers, P. Glans, D.L. Hansen, H. Wang, S.B. Whitfield, D.W. Lindle, R. Wehlitz, J.C. Levin, I.A. Sellin, and R.C.C. Perera

Accelerator and Fusion Research Division

May 1997
Submitted to
Physics Review Letters

LBNL-40415
LSBL-386
UC-410

BREAKDOWN OF THE INDEPENDENT PARTICLE APPROXIMATION IN HIGH-ENERGY PHOTOIONIZATION*

E.W.B. Dias, H.S. Chakraborty, P.C. Deshmukh, S.T. Manson,
O. Hemmers, P. Glans, D.L. Hansen, H. Wang, S.B. Whitfield,
D.W. Lindle, R. Wehlitz, J.C. Levin, I.A. Sellin, R.C.C. Perera

*This work was supported by the Director, Office of Energy Research, Office of Basic Energy Sciences, Materials Sciences Division, of the U.S. Department of Energy, under Contract No. DE-AC03-76SF00098.

BREAKDOWN OF THE INDEPENDENT PARTICLE APPROXIMATION IN HIGH-ENERGY PHOTOIONIZATION

E. W. B. Dias, H. S. Chakraborty, P. C. Deshmukh

Department of Physics, Indian Institute of Technology - Madras, Madras 600036, INDIA

Steven T. Manson

Department of Physics and Astronomy, Georgia State University, Atlanta, Georgia 30303

O. Hemmers, P. Glans, D. L. Hansen, H. Wang, S. B. Whitfield, D. W. Lindle

Department of Chemistry, University of Nevada, Las Vegas, NV 89154-4003

R. Wehlitz, J. C. Levin, I. A. Sellin

Department of Physics and Astronomy, University of Tennessee, Knoxville, TN 37996-1200

R. C. C. Perera

Advanced Light Source, Lawrence Berkeley laboratory, Berkeley, CA 94720

The independent particle approximation is shown to break down for the photoionization of both inner and outer $n\ell$ ($\ell > 0$) electrons of all atoms, at high enough energy, owing to interchannel interactions with the nearby ns photoionization channels. The effect is illustrated for Ne 2p in the 1 keV photon energy range through a comparison of theory and experiment. The implications for x-ray photoelectron spectroscopy of molecules and condensed matter is discussed.

The response of physical systems to ionizing electromagnetic radiation, photoionization, is a basic process of nature. Because of the weak coupling between incident photons and target electrons, the electromagnetic radiation exerts only a small perturbation on the target, thereby allowing the unambiguous study of target electron properties, e.g., correlation and many-body aspects of electron dynamics. In addition, the photoionization process, along with associated spectroscopies including photoelectron spectroscopy, is of importance in a variety of applications [1] including structural determination in crystalline solids, astrophysical modelling, radiation physics, etc. Owing to its importance, the field has seen a recent upsurge of activity, particularly in the x-ray range, due to the development of third generation synchrotron radiation sources on the experimental side [2], along with the dramatic increase in computer power available, on the theoretical side.

In recent years, a wide variety of studies, both theoretical and experimental, have shown the importance of correlation in the form of interchannel coupling on the photoionization process in the region of the outer shell thresholds [3-10]; in some cases, the single particle viewpoint breaks down completely. An outstanding example is the threshold behavior of Xe 5s which is completely dominated by interchannel coupling with the 5p and 4d channels [5]. In addition, in the vicinity of inner shell thresholds, dramatic effects are seen in outer shell cross sections due to interchannel coupling. Examples of this phenomenon abound [7], e.g., effects on the outer shell cross sections of atomic Ba in the vicinity of the 4d threshold [11]. It is generally thought, however, that in the x-ray range (far from the first ionization potential) away from inner shell ionization thresholds, the photoionization process can be well-characterized in a single channel

[3,7,12,13], or independent particle approximation, theory which omits correlation entirely. If this assertion is not true, then doubt is cast upon the interpretation of a number of studies of atoms, molecules and condensed matter involving x-ray photoabsorption.

In this paper it is shown that this notion is *not* true for the photoionization of *any* $n\ell$ ($\ell > 0$) subshell at high enough energy, but is true for ns subshell photoionization. To understand why this occurs, we first scrutinize the basic idea of interchannel coupling in some detail. Consider a simple situation where, within the framework of an independent particle theory (such as Hartree-Fock), the ground state of the target system is characterized by ψ_i and there are two final channels with wave functions $\psi_{1,\varepsilon}$ and $\psi_{2,\varepsilon}$ with ε the total energy; all of these wave functions being eigenfunctions of H_0, an approximation to the exact Hamiltonian of the system, H. For simplicity, we shall assume that there is no *intra*channel coupling, i.e.,

$$\langle \psi_{j,\varepsilon} | H | \psi_{j,\varepsilon'} \rangle = \varepsilon \, \delta(\varepsilon - \varepsilon') \qquad (1)$$

which is a property of a Hartree-Fock theory [14]. Now, consider a transition process under the action of transition operator T, and define the transition matrix elements

$$D_j(\varepsilon) = \langle \psi_i | T | \psi_{j,\varepsilon} \rangle, \quad j = 1,2. \qquad (2)$$

The "real" wave functions for the final states, the eigenfunctions of H, can be constructed as linear combinations of the $\psi_{1,\varepsilon}$'s and the $\psi_{2,\varepsilon}$'s. Using first order perturbation theory to approximate the "exact" wave functions, as modified to deal with the continuum [14], we obtain for the corrected wave functions

$$\Psi_{1,E} = \psi_{1,E} + \wp\int \frac{\langle \psi_{2,\varepsilon} | H-H_0 | \psi_{1,E} \rangle}{E - \varepsilon} \psi_{2,\varepsilon}\, d\varepsilon , \qquad (3a)$$

$$\Psi_{2,E} = \psi_{2,E} + \wp\int \frac{\langle \psi_{1,\varepsilon} | H-H_0 | \psi_{2,E} \rangle}{E - \varepsilon} \psi_{1,\varepsilon}\, d\varepsilon , \qquad (3b)$$

where $\wp$ represents the principal value. The perturbed matrix elements then become

$$M_1(E) = D_1(E) + \wp\int \frac{\langle \psi_{2,\varepsilon} | H-H_0 | \psi_{1,E} \rangle}{E - \varepsilon} D_2(\varepsilon)\, d\varepsilon , \qquad (4a)$$

$$M_2(E) = D_2(E) + \wp\int \frac{\langle \psi_{1,\varepsilon} | H-H_0 | \psi_{2,E} \rangle}{E - \varepsilon} D_1(\varepsilon)\, d\varepsilon . \qquad (4b)$$

These equations embody the notion of interchannel coupling, i.e., the transition matrix element of each channel being modified owing to the fact that the "real" wave functions of the system involve a mixture of channels. For example, for electric dipole photoionization of Xe 5s, let channel 1 be 5s $\rightarrow$ kp and channel 2, 5p $\rightarrow$ kd. Eq.(4a) then becomes

$$M_{5s\rightarrow kp}(E) = D_{5s\rightarrow kp}(E) + \wp\int \frac{\langle \psi_{5p\rightarrow k'd} | H-H_0 | \psi_{5s\rightarrow kp} \rangle}{E - \varepsilon} D_{5p\rightarrow k'd}(\varepsilon)\, d\varepsilon . \qquad (5)$$

Because these channels are degenerate, the denominator, E - ε, can vanish. Further, the interaction matrix element in the numerator of Eq.(5), essentially a matrix element of e^2/r_{ij}, is not small. Thus, since $D_{5p\rightarrow kd}$ is much larger than $D_{5s\rightarrow kp}$, the integral term in Eq.(5) dominates the matrix element over a broad range above the 5s ionization threshold. Significant effects attributable to this behavior is confirmed by experiment [5].

Similarly, in the photoionization of Ba 6s around the 4d ionization threshold, the dipole matrix element becomes

$$M_{6s\to kp}(E) = D_{6s\to kp}(E) + \mathcal{P}\int \frac{\langle \Psi_{4d\to k'f} | H-H_0 | \Psi_{6s\to kp}\rangle}{E-\varepsilon} D_{4d\to k'f}(\varepsilon)\, d\varepsilon \qquad (6)$$

and the second term dominates, just like Xe 5s, because $D_{4d \to kf}$ is much larger than $D_{6s \to kp}$. There is, however, a difference in the two cases. In the latter case, the second term dominates only in a limited range around the 4d threshold. For energies below the threshold, the second term falls off rapidly due to the energy denominator. Above the threshold, it falls off because the interaction matrix element decreases with increasing energy as a result of the destructive interference between the continuum waves of the two channels which have rather different energy for a given hυ. Only near the 4d threshold, where the kf wave function is not very oscillatory, is the interaction matrix element large. In the Xe 5s case, by contrast, because the 5s and 5p have roughly the same binding energy, the continuum waves remain roughly "in phase" at all energies so that the interaction matrix element falls off only very slowly with energy and the interchannel coupling effects persist over a large energy range.

Now, consider the photoionization of an np electron, inner or outer, from any atom, molecule or solid. Not far above the np ionization threshold will always be an ns threshold. Thus, a bit above the np threshold, there will always be an ns cross section degenerate with the np cross section. However, no matter what the relative values of these cross sections are near the thresholds, at energies far above threshold the ns cross section will *always* dominate the np. This is because, at high energy, the electric dipole photoionization cross section for an $n\ell$ subshell falls off with energy as $E^{-(7/2+\ell)}$ [3,7]. Thus, using Eqs.(4),

$$M_{np\rightarrow kd(s)}(E) = D_{np\rightarrow kd(s)}(E) + \mathcal{P}\int \frac{\langle \Psi_{ns\rightarrow k'p} | H-H_0 | \Psi_{np\rightarrow kd(s)} \rangle}{E-\varepsilon} D_{ns\rightarrow k'p}(\varepsilon)\, d\varepsilon . \quad (7)$$

Because the energies of the photoelectrons from the np and ns channels are similar, the interaction matrix element falls off only very slowly and remains large with increasing energy, much like the Xe 5s case. Thus, for both np $\rightarrow$ kd and np $\rightarrow$ ks, the second term in Eq.(7) becomes a larger and larger contribution to the matrix element, with increasing energy. This is in sharp contradistinction to the notion that the single-particle characteristics of the electric dipole photoionization process dominate at high energy.

As a prototypical example, consider the photoionization of atomic Ne in the 1 keV photon energy range. Calculations were performed within the framework of the relativistic-random-phase approximation (RRPA) [15,16] for the cross section, σ, and photoelectron angular distribution asymmetry parameter, β, of the 2p subshell. Four levels of approximation were considered: (i) coupling of all of the relativistic single excitation channels arising from 2p, 2s and 1s; (ii) from 2p and 2s only; (iii) from 2p and 1s only; (iv) from 2p alone and 2s alone.

The results for the 2p partial cross section of Ne are shown in Figs. 1 and 2. From these results, it is seen that the calculation predicts that all four levels of calculation agree rather well at the lowest energies considered. This is because the 2p cross section dominates the 2s cross section in this energy range by a factor of about six, so that interchannel coupling does not appreciably affect the 2p matrix elements. With increasing photon energy, however, the 2p matrix elements fall off more rapidly than the 2s, so that by the 500 eV range, the 2s cross section is larger than the $2p_{3/2}$ by a factor of two and larger than the $2p_{1/2}$ by a factor of more

than three. This translates into two groups of results in this energy range as seen in Fig. 1. The two calculations with 2p and 2s coupled agree with each other, and the other two agree with each other but disagree with the first group. This clearly points to the interchannel coupling between 2p and 2s channels being responsible for this difference. With increasing energy, this behavior is interrupted as we approach 870 eV where the 1s channels open and coupling with them becomes crucial, as seen in Figs. 1 and 2. Above 1000 eV, however, we are back to the same two groups of curves, just as in the 500 eV region, indicating that in this region as well, it is the coupling of the 2p with the 2s channels that matters. The coupling produces a 2p cross section more than 30% above the uncoupled result, as seen in Fig. 2.

New measurements have been made for the ratio of the 2s to the 2p cross section, which take into account the non-dipole contribution to the photoelectron angular distribution [17], and they are shown in Fig. 3, along with our theoretical results. These measurements confirm the accuracy of the calculation by the excellence of the agreement. But the most important result demonstrated by Fig. 3 is the divergence between the fully coupled and the uncoupled calculations at the highest energies; and the fact that it is the coupling with 2s that is important as evidenced by the agreement between the full (2p + 2s + 1s) calculation and the 2p + 2s calculation. In addition, a central field calculation [3,12,13] was performed using a Hartree-Slater potential [18] and the results (not shown) are virtually identical to the uncoupled 2p RRPA result of Fig. 3, as expected. Thus, it is clear that the single-particle result does not agree with experiment at the higher energies, while the coupled result does, in contrast to the conventional wisdom [3,7,12,13].

Looking at the photoelectron angular distribution parameter, β, the experimental results

[17] along with the various levels of calculated results, are shown in Fig. 4; all levels of calculation agree reasonably well at the lowest energies, the separation into the same two groups occurs with increasing energy is seen, and the agreement of the experimental results with the full RRPA calculation is clear. Our single particle result for β (not shown) also is virtually indistinguishable from the 2p alone calculation. At the highest energies considered, we see about a 30% shift in β from the single particle calculation, reiterating the point that even out at 1.5 keV, approximately 100 times the threshold energy, interchannel coupling does matter.

This interchannel coupling effect should also be in evidence for nd and nf subshells as well, by the arguments presented. In addition, although the detailed example was for an atom, the arguments are exactly the same for molecular and condensed matter targets. One *caveat* should be mentioned, however. At extremely high energies (tens of keV or higher), where relativistic interactions take over [19-21], the photoionization cross sections no longer behave as $E^{-(7/2+\ell)}$ and these arguments no longer apply. But for a very significant energy region below that, they do.

In conclusion, we have shown that the high energy photoionization of all $n\ell$ ($\ell > 0$) subshells will exhibit a breakdown of the independent particle approximation owing to the effect of interchannel coupling with the nearby ns channels, and this effect has been demonstrated for Ne 2p employing both theory and experiment. It is predicted that the same effect applies equally to molecules and condensed matter, as well as atoms.

This work was supported by the National Science Foundation, NASA, the Department of Energy, the Research Corporation and the Petroleum Research Fund. The authors thank the staff of the ALS for their support and the IBM, LBNL, LLNL, University of Tennessee and Tulane

University collaboration for beam time at beamline 8.0.

REFERENCES

1. H. S. W. Massey, E. W. McDaniel and B. Bederson, eds., *Applied Atomic Collision Physics* (Academic Press, NY, 1983), 5 volumes.

2. A. S. Schlachter and F. J. Wuilleumier, eds., *New Directions in Research with Third Generation Soft X-Ray Sources* (Kluwer, Dordrect, Netherlands, 1992), NATO ASI Series E, Vol. 254.

3. A. F. Starace, in *Handbuch der Physik*, Vol. 31, ed. by W. Mehlhorn (Springer-Verlag, Berlin, 1982), pp. 1-121.

4. J. A. R. Samson, in *Handbuch der Physik*, Vol. 31, ed. by W. Mehlhorn (Springer-Verlag, Berlin, 1982), pp. 123-213.

5. V. Schmidt, Rep. Prog. Phys. **55**, 1483 (1992).

6. B. Sonntag and P. Zimmermann, Rep. Prog. Phys. **55**, 911 (1992).

7. M. Ya. Amusia, *Atomic Photoeffect* (Plenum Press, NY, 1990).

8. T.-N. Chang, ed., *Many-Body Theory of Atomic Structure and Photoionization* (World Scientific, Singapore, 1993).

9. J. Berkowitz, *Photoabsorption, Photoionization, and Photoelectron Spectroscopy* (Academic Press, NY, 1979).

10. H. P. Kelly, in *X-Ray and Inner-Shell Processes*, ed. by T. A. Carlson, M. O. Krause and S. T. Manson (American Institute of Physics, NY, 1990), pp. 292-314.

11. J. M. Bizau, D. Cubaynes, P. Gerard and F. J. Wuilleumier, Phys. Rev. A **40**, 3002 (1989).

12. S. T. Manson and D. Dill, in *Electron Spectroscopy*, ed. by C. R. Brundle and A. D. Baker (Academic Press, NY, 1978), Vol. 2, pp. 157-195.

13. S. T. Manson, Adv. Electronics Electron Phys. **41**, 73 (1976).

14. U. Fano, Phys. Rev. A **124**, 1866 (1961).

15. W. R. Johnson and C. D. Lin, Phys. Rev. A **20**, 964 (1979).

16. W. R. Johnson, C. D. Lin, K. T. Cheng and C. M. Lee, Phys. Scripta **21**, 409 (1980).

17. O. Hemmers, G. Fisher, P. Glans, D. L. Hansen, H. Wang, S. B. Whitfield, D. W. Lindle, R. Wehlitz, J. C. Levin, I. A. Sellin, R. C. C. Perera, E. W. B. Dias, H. S. Chakraborty, P. C. Deshmukh and S. T. Manson, Phys. Rev. Letters (submitted).

18. F. Herman and S. Skillman, *Atomic Structure Calculations*, (Prentice-Hall, Englewood Cliffs, N.J., 1963).

19. R. H. Pratt, A. Ron and H. K. Tseng, Rev. Mod. Phys. **45**, 273 (1973).

20. I. P. Grant, J. Phys. B **7**, 1458 (1974).

21. A. Ron, I. B. Goldberg, J. Stein, S. T. Manson, R. H. Pratt and R. Y. Yin, Phys. Rev. A **50**, 1312 (1994).

FIGURE CAPTIONS

1. Photoionization cross section for Ne 2p between 200 eV and 800 eV. The curves are relativistic random phase approximation (RRPA) results with the single excitation channels arising from 2p, 2s and 1s coupled (solid curve); 2p and 2s (dash curve); 2p and 1s (dash-dot curve); and 2p alone (dot curve).

2. Photoionization cross section for Ne 2p between 800 eV and 1500 eV. The curves are relativistic random phase approximation (RRPA) results with the single excitation channels arising from 2p, 2s and 1s coupled (solid curve); 2p and 2s (dash curve); 2p and 1s (dash-dot curve); and 2p alone (dot curve).

3. Ratio of the 2s to 2p cross section for Ne. The calculations employed the RRPA formalism with the single excitation channels arising from 2p, 2s and 1s coupled (solid curve); 2p and 2s coupled (dash curve); and 2p and 2s *uncoupled* to each other (dot curve). The experimental points were measured in the manner discussed in Ref. 17.

4. Photoelectron angular distribution asymmetry parameter, β, for Ne 2p calculated using the RRPA formalism with the single excitation channels arising from 2p, 2s and 1s coupled (solid curve); 2p and 2s (dash curve); 2p and 1s (dash-dot curve); and 2p alone (dot curve). The experimental points are from Ref. 17 augmented by some new points reported here using the methodology of Ref. 17.

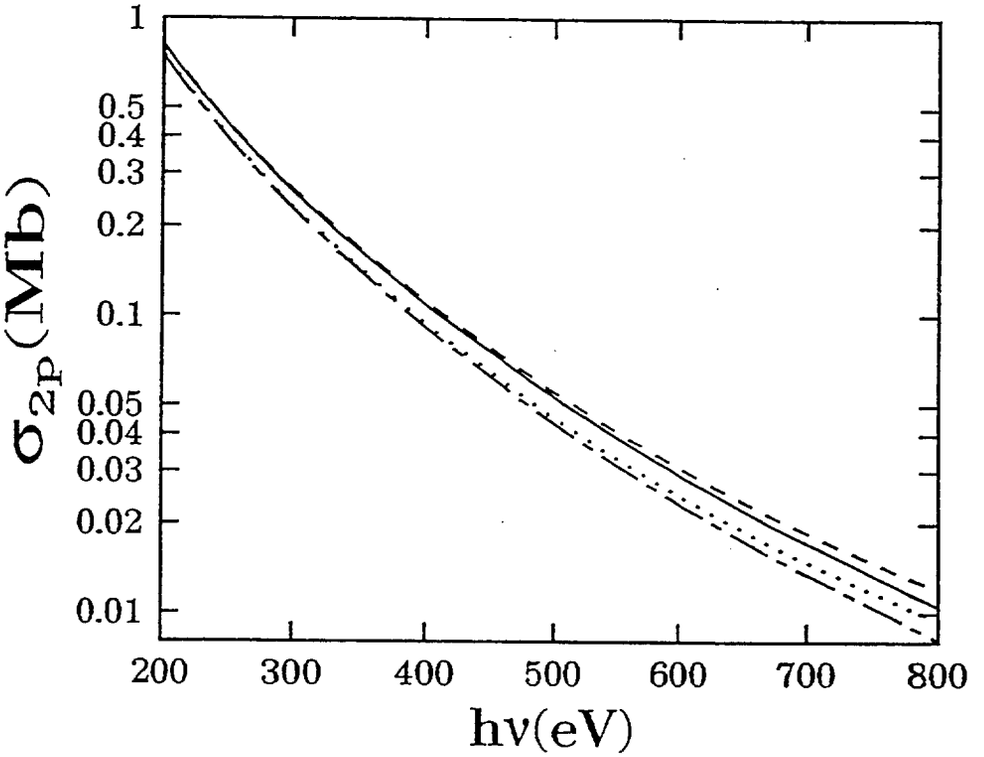
1
0.5
0.4
0.3
0.2
0.1
0.05
0.04
0.03
0.02
0.01
σ2p(Mb)
200
300
400
500
600
700
800
hν(eV)

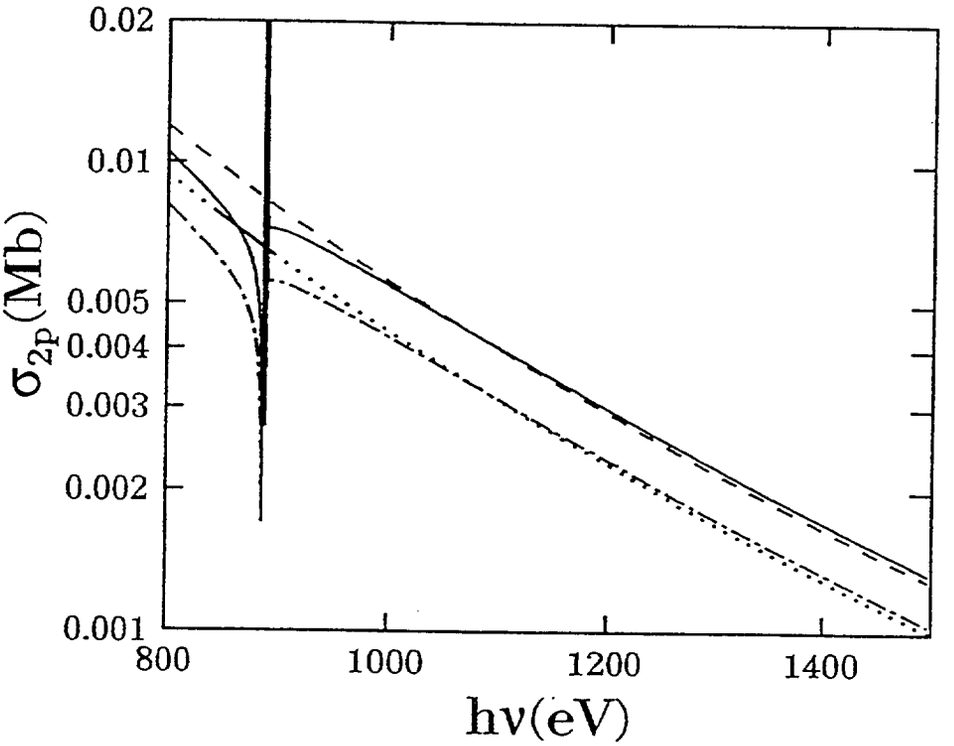
0.02
0.01
0.005
0.004
0.003
0.002
0.001
σ_{2p}(Mb)
800
1000
1200
1400
hν(eV)

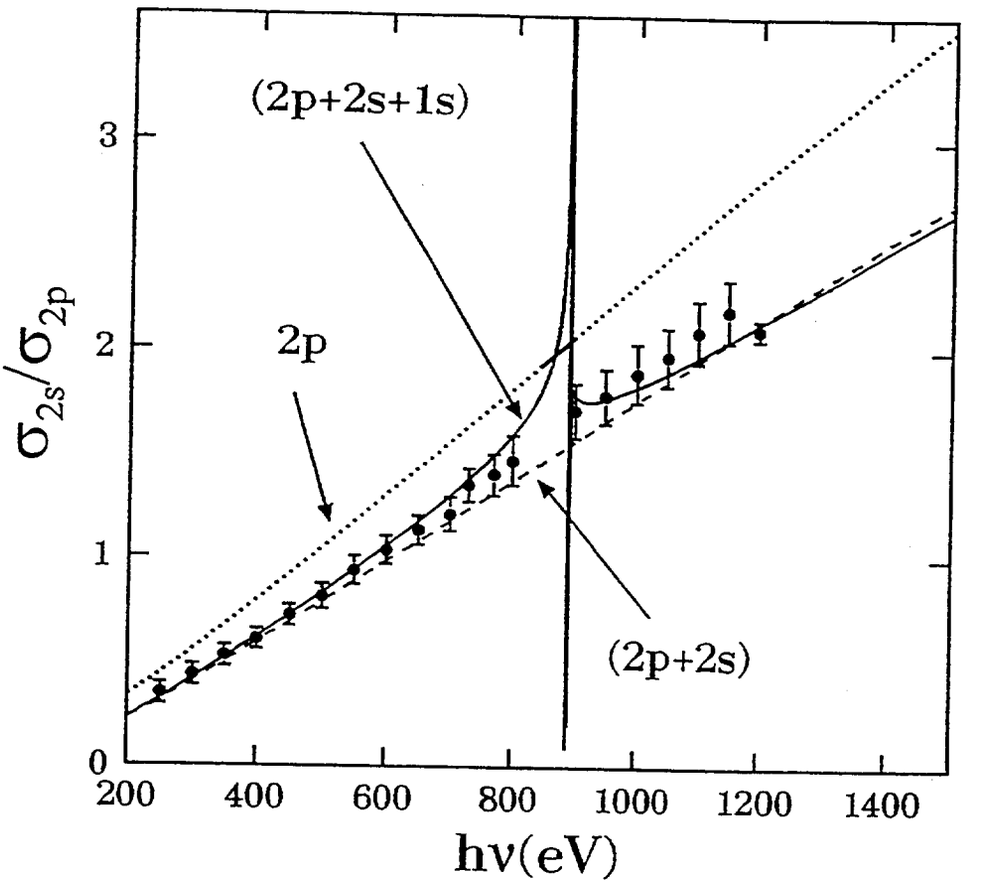
(2p+2s+1s)
2p
(2p+2s)
σ_{2s}/σ_{2p}
hν(eV)
0
1
2
3
200
400
600
800
1000
1200
1400

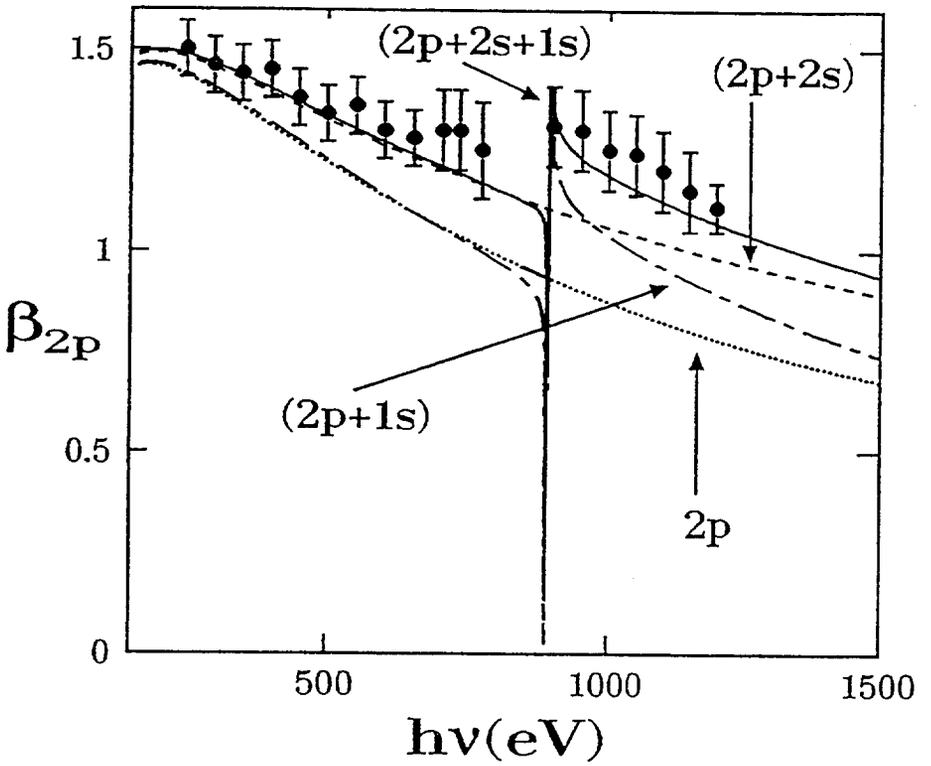
1.5
1
0.5
0
β_{2p}
(2p+2s+1s)
(2p+2s)
(2p+1s)
2p
500
1000
1500
hν(eV)